Schwinger-boson approach to the kagome antiferromagnet with Dzyaloshinskii-Moriya interactions: Phase diagram and dynamical structure factors

L. Messio,[1] O. Cépas,[2] and C. Lhuillier[1]

[1]*Laboratoire de physique théorique de la matière condensée, UMR 7600 CNRS, Université Pierre-et-Marie-Curie-Paris 6, 75252 Paris Cedex 05, France*

[2]*Institut Néel, CNRS et Université Joseph Fourier, BP 166, F-38042 Grenoble Cedex 9, France*

We have obtained the zero-temperature phase diagram of the kagomé antiferromagnet with Dzyaloshinskii-Moriya interactions in Schwinger-boson mean-field theory. We find quantum phase transitions (first or second order) between different topological spin-liquid and Néel-ordered phases (either the $\sqrt{3} \times \sqrt{3}$ state or the so-called $\mathbf{Q}=0$ state). In the regime of small Schwinger-boson density, the results bear some resemblances with exact diagonalization results and we briefly discuss some issues of the mean-field treatment. We calculate the equal-time structure factor (and its angular average to allow for a direct comparison with experiments on powder samples), which extends earlier work on the classical kagomé to the quantum regime. We also discuss the dynamical structure factors of the topological spin-liquid and the Néel-ordered phases.

I. INTRODUCTION

The Dzyaloshinskii-Moriya (DM) interactions[1] are inevitably present in $S=1/2$ magnetic oxides when the magnetic bonds lack inversion centers, which is the case of the kagome lattice. Although small in strength (it originates in the spin-orbit coupling), such a correction may favor other phases than the ones usually predicted by using the standard Heisenberg model. By breaking explicitly the spin-rotation symmetry of the system, the Dzyaloshinskii-Moriya forces tend to reduce the spin fluctuations and may therefore be detrimental to the long-searched spin-liquid phases. However, would the Heisenberg phase be gapped, such as in valence bond crystals (generalized spin-Peierls states) or in topological spin liquids (TSLs),[2–4] then it would be robust against perturbations typically smaller than the gap. An example is given by the Shastry-Sutherland compound SrCu$_2$(BO$_3$)$_2$ which remains in the singlet phase in the presence of Dzyaloshinskii-Moriya couplings.[5] In the kagome antiferromagnet (with pure nearest-neighbor Heisenberg interaction), the very existence of a gap remains an open question,[6] algebraic spin-liquid and gapless vortex phases have been proposed as alternatives in the recent years.[7–9] Current numerical estimates of the gap provide a small upper bound $\sim 0.05J$.[6,10–13] In any case the gap (if it exists) could be smaller than the Dzyaloshinskii-Moriya coupling (especially in copper oxides where it is typically $\sim 0.1J$) and the latter is therefore particularly relevant. Experiments on the kagome compound ZnCu$_3$(OH)$_6$Cl$_3$ (Refs. 14–17) have found no spin gap (despite a temperature much lower than the upper estimation of the gap) but the chemical disorder[18–20] and, precisely, the existence of Dzyaloshinskii-Moriya interactions[21–24] make the spin gap issue not yet clear.

In fact, the Dzyaloshinskii-Moriya interactions were argued to induce long range $\mathbf{Q}=0$, 120° Néel order in the kagome antiferromagnet: the algebraic spin-liquid theory predicts the instability at a critical strength $D_c=0$ (Ref. 25) while there is a finite quantum critical point at $D_c \sim 0.1J$ in

exact diagonalization results on samples of size up to $N=36$.[23] Since it is clear that there is no Néel order at D strictly zero[10,26] and there is Néel order for D large enough,[23] it is tempting to tackle the problem using the Schwinger-boson representation for the spin operators.[27] Indeed this approach allows in principle to capture both topological spin-liquid and Néel-ordered phases[28] and offers a first framework to describe this quantum phase transition. The caveat is that the actual Schwinger-boson mean-field solution for the $S=1/2$, $D=0$ kagome antiferromagnet is already long-ranged ordered (LRO) and it is only at smaller values of S (which in this approach is a continuous parameter) that a disordered spin-liquid phase is stabilized. This result may however be an artifact of the mean-field approach and it is possible that fluctuations not taken into account at this level do stabilize the disordered phase for the physical spin-1/2 system. It is therefore interesting to see what phases the Schwinger-boson mean-field theory predicts for the kagome antiferromagnet perturbed by Dzyaloshinskii-Moriya interactions.

In Sec. II we present the model and the method. In Sec. III we discuss the phase diagram together with general ground-state properties. In Sec. IV, we illustrate the evolution of observables across the quantum phase transition from topological spin liquid to long-ranged Néel order: the spinon spectrum, the gap, the order parameter, and the condensed fraction of bosons. We calculate the equal-time structure factor, its powder average, and briefly compare both to classical calculation and experimental results. In Sec. V we present the dynamical spin structure factor and its behavior in the two phases. We also describe how these behaviors emerge from the properties of the spinon spectrum.

II. MODEL

We have considered additional DM interactions to the standard Heisenberg model on the kagome lattice

$$H = \sum_{\langle i,j \rangle} [J\mathbf{S}_i \cdot \mathbf{S}_j + \mathbf{D}_{ij} \cdot (\mathbf{S}_i \times \mathbf{S}_j)], \qquad (1)$$

where $\langle i,j \rangle$ stands for nearest neighbors (each bond is counted once) and $\mathbf{S}_i$ is a quantum spin operator on site i, the
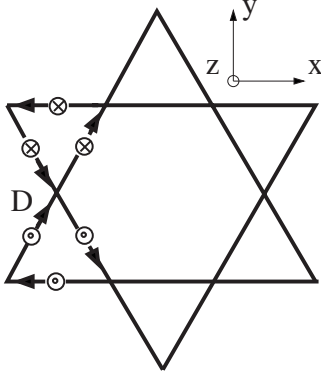
FIG. 1. The Dzyaloshinskii-Moriya field in the model (spin rotated frame—see text).

Dzyaloshinskii-Moriya field $\mathbf{D}_{ij}$ is taken to be along the z axis and is staggered from up to down triangles (see Fig. 1). For this, we work in a rotated frame which allows to eliminate the other components (the $\mathbf{S}_i$ are to be viewed as rotated operators).[23] In this case, the Dzyaloshinskii-Moriya field favors a vector chirality along z and the model (1) has a global U(1) symmetry which can be spontaneously broken or not.

The Schwinger-boson representation is written

$$\mathbf{S}_i = \frac{1}{2}(a_i^\dagger \quad b_i^\dagger)\sigma\begin{pmatrix} a_i \\ b_i \end{pmatrix} \quad n_i \equiv a_i^\dagger a_i + b_i^\dagger b_i = 2S, \qquad (2)$$

where $a_i^\dagger$ (respectively, $b_i^\dagger$) creates a boson on site i with spin $\uparrow$ (respectively, $\downarrow$) and σ are the Pauli matrices. To fix the length of the spin, $\mathbf{S}_i^2 = (n_i/2)(n_i/2+1) = S(S+1)$, we need to have $n_i = 2S$ bosons per site. We define the bond creation operator

$$A_{ij}^\dagger \equiv \frac{1}{2}(e^{i\theta_{ij}}a_i^\dagger b_j^\dagger - e^{-i\theta_{ij}}b_i^\dagger a_j^\dagger) \qquad (3)$$

with $\theta_{ij} = D_{ij}/(2J)$. A similar approach has been developed by Manuel et al.[29] on the square lattice. With this definition and up to small corrections of order D_{ij}^2/J, the model takes its standard form[27]

$$H = -2J\sum_{\langle i,j \rangle} A_{ij}^\dagger A_{ij} + NzJS^2/2, \qquad (4)$$

where N is the number of lattice sites and $z=4$ the coordination number. H has a local U(1) gauge symmetry: it is invariant under $(a_i, b_i) \rightarrow (e^{i\alpha_i}a_i, e^{i\alpha_i}b_i)$, where $\alpha_i \in [0, 2\pi]$. Applied to the vacuum of boson, $A_{ij}^\dagger$ creates a superposition of a singlet and a triplet state on the ij bond, i.e., the exact ground state of a single bond of Eq. (4). In mean-field theory,[27,30] the quartic Hamiltonian (4) is replaced by a self-consistent quadratic Hamiltonian with a bond varying order parameter $\mathcal{A}_{ij} \equiv \langle A_{ij} \rangle$ and the constraint $n_i = 2S$ enforced on average with Lagrange multipliers λ_i. Up to a constant the mean-field Hamiltonian reads
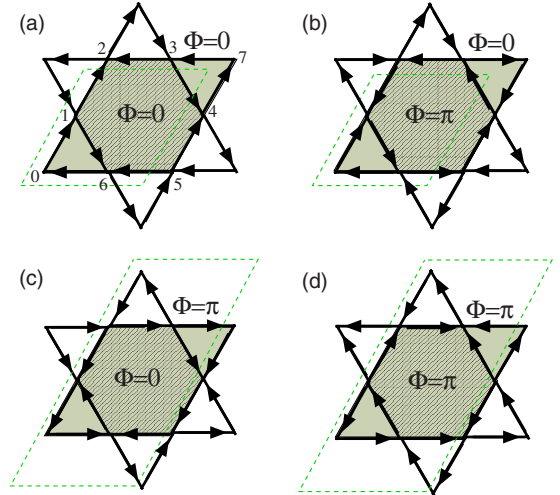

FIG. 2. (Color online) The bond order parameter $\mathcal{A}_{ij}$ of the four symmetric *Ansätze* of model Eq. (1). Its modulus $\mathcal{A}$ is a constant for all bonds, an arrow from i to j means $\mathcal{A}_{ij} > 0$. The fluxes through the hexagon and the rhombus (Φ_{Hex}, Φ_{Rho}) are in (a) $(0,0)$, (b) $(\pi, 0)$, (c) $(0, \pi)$, and (d) (π, π). The unit cell is shown by dashed lines (twice larger for the last two *Ansätze*).

$$H_{MF} = -2J\sum_{\langle i,j \rangle} \mathcal{A}_{ij}^* A_{ij} + A_{ij}^\dagger \mathcal{A}_{ij} - |\mathcal{A}_{ij}|^2 - \sum_i \lambda_i(n_i - 2S). \qquad (5)$$

We now restrict our search to solutions whose physical (thus gauge invariant) observables do not break the space-group symmetry of the Hamiltonian and hence could realize spin-liquid states. There are only four classes of such states (called *Ansätze* in Refs. 28 and 31 and in the following), labeled by their projective symmetry group,[31] or equivalently by fluxes around hexagons and rhombus (Φ_{Hex}, Φ_{Rho}) $= (0,0)$, $(\pi, 0)$, $(0, \pi)$, or (π, π). The flux Φ around a loop $(i_1, i_2, \ldots, i_{2n})$ with an even number of links is defined by[32]

$$Ke^{i\Phi} = \mathcal{A}_{12}(-\mathcal{A}_{23}^*), \ldots, \mathcal{A}_{2n-1,2n}(-\mathcal{A}_{2n,1}^*). \qquad (6)$$

It is a gauge-invariant quantity. In each of the four *Ansätze*, all $\mathcal{A}_{ij}$ have the same amplitude $|\mathcal{A}_{ij}| = \mathcal{A}$ and are real in a well chosen gauge. Their signs are represented on Fig. 2. These four *Ansätze* are identical to those obtained by Wang and Vishwanath for the kagome Heisenberg model: they are fully determined by rotational and translational invariances of the spin Hamiltonian on the lattice. Note that to be invariant under the lattice symmetries, the bosonic Hamiltonian of these *Ansätze* must be gauge transformed, which does not modify the corresponding spin Hamiltonian. That explains the noninvariance of these *Ansätze* under the lattice symmetries. The $(0,0)$ *Ansatz* corresponds to the $\sqrt{3} \times \sqrt{3}$ state and the $(\pi, 0)$ *Ansatz* to the $\mathbf{Q}=0$ state, originally found by Sachdev[28] while the last two involve larger unit cells and may as well be relevant for longer range interaction or ring exchange.[31,33]

Using the translation symmetry of the mean-field *Ansätze*, the Hamiltonian is Fourier transformed,

$$H_{MF} = \sum_{\mathbf{q}} \phi_{\mathbf{q}}^{\dagger} N_{\mathbf{q}} \phi_{\mathbf{q}} + NJz\mathcal{A}^2 + (2S+1)N\lambda \qquad (7)$$

with

$$\phi_{\mathbf{q}}^{\dagger} \equiv [(a_{1\mathbf{q}})^{\dagger}, \dots, (a_{m\mathbf{q}})^{\dagger}, b_{1-\mathbf{q}}, \dots, b_{m-\mathbf{q}}], \qquad (8)$$

$$a_{i\mathbf{q}} \equiv \frac{1}{\sqrt{N/m}} \sum_{\mathbf{x}} e^{-i\mathbf{qx}} a_{i\mathbf{x}} \qquad (9)$$

(the same for the $b_{i\mathbf{q}}$ operators), where m is the number of sites in the unit cell: $m=3$ for the first two *Ansätze* and $m=6$ for the second two. A given site is defined by a sublattice $i \in [1,m]$ and unit-cell $\mathbf{x}$ indices. $N_{\mathbf{q}}$ are $2m \times 2m$ matrices whose coefficients depend on $\mathcal{A}$, λ, $\mathbf{q}$, and of the *Ansatz*. The Hamiltonian is diagonalized using a numerically constructed[34] Bogoliubov transformation

$$\phi_{\mathbf{q}} = P_{\mathbf{q}} \tilde{\phi}_{\mathbf{q}} \quad P_{\mathbf{q}} = \begin{pmatrix} U_{\mathbf{q}} & -V_{\mathbf{q}} \\ V_{\mathbf{q}} & U_{\mathbf{q}} \end{pmatrix}, \qquad (10)$$

where $U_{\mathbf{q}}$ and $V_{\mathbf{q}}$ are $m \times m$ matrices,

$$H_{MF} = \sum_{\mathbf{q}\mu} \omega_{\mathbf{q}\mu} \tilde{\phi}_{\mathbf{q}\mu}^{\dagger} \tilde{\phi}_{\mathbf{q}\mu} + NJz\mathcal{A}^2 + (2S+1)N\lambda, \qquad (11)$$

where $\omega_{\mathbf{q}\mu}$ is the dispersion relation of the $\mu = 1, \dots, 2m$ spinon modes. Each mode is twice degenerate because of the time-reversal symmetry. The ground state $|\tilde{0}\rangle$ is the vacuum of the Bogoliubov bosons. At zero temperature, $\mathcal{A}$ and λ are determined by extremizing the total energy, subject to the constraints,

$$\mathcal{A} = |\langle A_{ij} \rangle| \quad \langle n_i \rangle = 2S \qquad (12)$$

[the energy is in fact a saddle point, minimum in $\mathcal{A}$ and maximum in λ (Ref. 35)].

III. PHASE DIAGRAM

To obtain the phase diagram, the two self-consistent Eq. (12) are implemented numerically for each of the four *Ansätze* of Fig. 2. The energies of the different *Ansätze* are shown in Fig. 3 versus $\theta = D/(2J)$ for three values of S: 0.025, 0.2, and 0.5. The corresponding full phase diagram of the model is shown in Fig. 4.

Before discussing the predictions of this model, let us remark that in the small S limit all these phases can in fact be captured by an analytic perturbative expansion in term of flux through closed loops.[32] At small S, the density of bosons is small and the constraints [Eq. (12)] imply that $\mathcal{A}$ must be small compared to λ. The mean-field energy can then be expanded in terms of gauge-invariant products of bond order parameters $\mathcal{A}_{ij}$ along closed loops. Following Tchernyshyov et al.,[32] we have computed the expansion up to loops of length 16 in order to calculate the energy difference between the four *Ansätze*. The results of these calculations give the low S phase boundaries (dashed lines superimposed to the exact results in Fig. 4). It is seen on this example that the so-called flux expulsion conjecture[32] which predicts that the ground state in nonfrustrated models has zero flux through
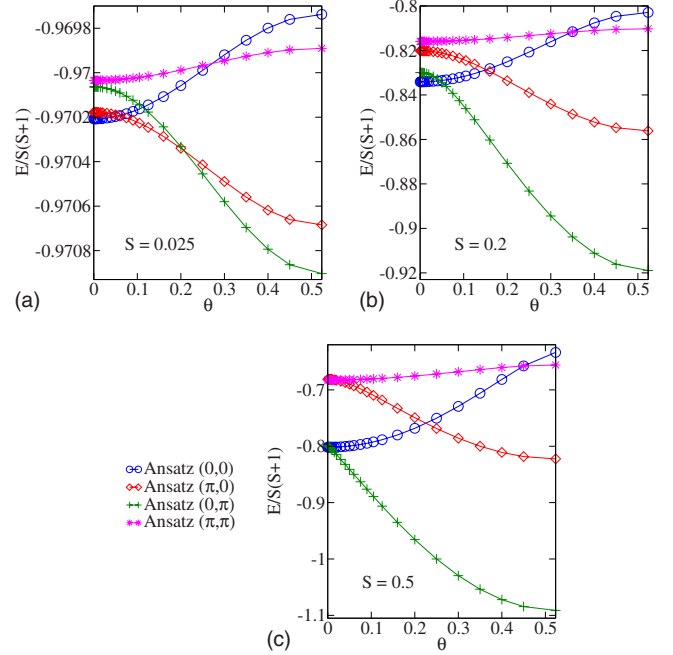

FIG. 3. (Color online) Ground state energies per site of the four *Ansätze* vs $\theta = D/2J$, for $S = 0.025$, 0.2, and 0.5.

any closed loop does not apply to frustrated problem, where the $(0,\pi)$ and $(\pi,0)$ appear as ground states in an extended range of parameters.

For the sake of clarity, we will first discuss the full phase diagram (Fig. 4). (We postpone to the next paragraph the illustration on the spinon spectrum of the differences between topological spin-liquid and Néel-ordered phases. Let us only mention at this stage that a spin-liquid phase is characterized by a fully gapped spinon spectrum, whereas in a Néel-ordered phase the spinon spectrum is gapless at the thermodynamic limit, as the magnon modes.) For $S = 1/2$, there is a direct first-order transition between the long-ranged Néel-ordered $\sqrt{3} \times \sqrt{3}$ and $\mathbf{Q} = 0$ phases for a finite
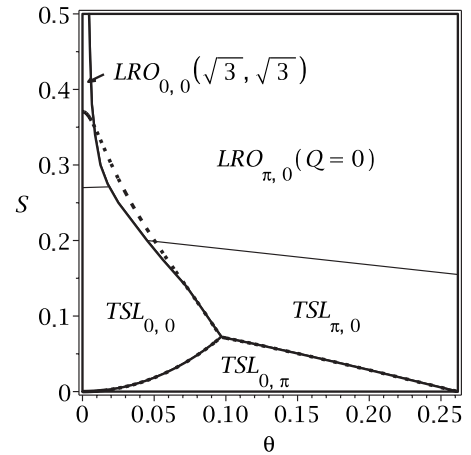

FIG. 4. Phase diagram at zero temperature [spin S, $\theta = D/(2J)$]: TSL and Néel LRO phases characterized by their fluxes through hexagons and rhombi. For larger S the region of existence of the $(0,0)$ phase shrinks. Dashed lines are the result of a perturbative expansion at small S (see text).

Dzyaloshinskii-Moriya coupling. This finite range of existence of the $\sqrt{3} \times \sqrt{3}$ phase shrinks with increasing values of the spin, which is fully compatible with the classical solution.[36]

For low S values, and increasing θ, Figs. 3 and 4 show a sequence of first-order transitions between the $(0,0)$ $(\sqrt{3} \times \sqrt{3}$ short-range fluctuations), $(0,\pi)$, and $(\pi,0)$ $(\mathbf{Q}=0$, short-range fluctuations) spin-liquid phases. [The (π,π) state is always at higher energy and never realized.] The $(0,\pi)$ state was argued to be stabilized by four-spin interactions up to a large critical S.[31] It also appears here in a small part of the phase diagram for very small S but first-order transitions prevent its stability at larger S.

In the absence of Dzyaloshinskii-Moriya coupling, the $S=1/2$ results of this approach are qualitatively not consistent with exact diagonalizations which point to a nonmagnetic phase. But in the range of parameters around $S \sim 0.2$, the $(\pi,0)$ Schwinger-boson mean-field results are qualitatively not very far from exact diagonalization results: there are short-ranged $\mathbf{Q}=0$ correlations in the Heisenberg case[12,37] and a second-order phase transition to 120° $\mathbf{Q}=0$ Néel order under the effect of Dzyaloshinskii-Moriya coupling.[23]

As already mentioned, it may be that a theory beyond mean field, with a better treatment of the constraint shifts the region $S \sim 0.2$ to the physically accessible $S=1/2$. Indeed in the Schwinger bosons mean-field approach it is well known[27] that there are large fluctuations of the number of bosons. As a consequence, the square of the spin operator

$$\langle \mathbf{S}_i^2 \rangle = S(S+1) + (\langle n_i^2 \rangle - \langle n_i \rangle^2)/4 \tag{13}$$

takes a value 3/2 times larger than $S(S+1)$ (at $D=0$).[38] The prefactor is even larger in the presence of Dzyaloshinskii-Moriya interaction and amounts to ~ 1.75 for $\theta=0.25$. From the physical spin-1/2 point of view, the mean-field approximation leads to (unwanted) extra fluctuations and, on average, the spin length is larger than assumed [because of (13)]. The SU(2) symmetry of the Heisenberg model can be generalized to $Sp(\mathcal{N})$ [which reduces to SU(2) when $\mathcal{N}=1$] by duplicating $\mathcal{N}$ times each pair (a_i, b_i) of boson operators: $(a_{i\alpha}, b_{i\alpha})$, where $\alpha=1 \cdots \mathcal{N}$ is a "flavor" index.[2] It can be shown that the different boson flavors decouple in the limit of large $\mathcal{N}$, leading to $\mathcal{N}$ uncorrelated copies of the single flavor problem, for which the *exact* solution is given by the present *mean-field* treatment of the $\mathcal{N}=1$ model. Thus, it is only in the $\mathcal{N}=\infty$ limit of the model that the mean-field treatment becomes exact and that the fixed "spin length" is recovered. However, the mean-field theory can describe qualitatively the magnetically ordered phases and the deconfined $\mathbb{Z}_2$ spin-liquid phases of the SU(2) model.[39]

IV. SPINON SPECTRUM AND QUANTUM PHASE TRANSITION FROM A TOPOLOGICAL SPIN-LIQUID TO A NÉEL-ORDERED PHASE

A. Spin-liquid phases (low S)

In the low S regime, the spinon spectrum of Eq. (11) is gapped everywhere. Figure 5 (left) gives a typical example
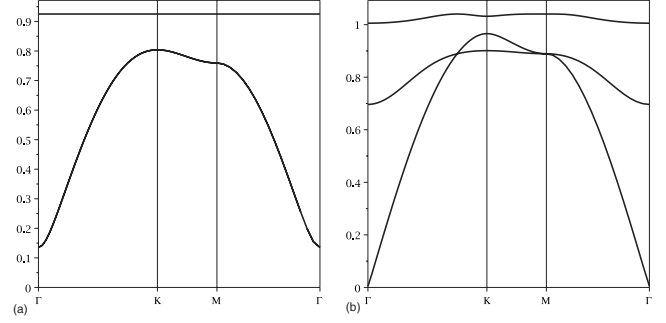

FIG. 5. Spinon dispersions along Γ-K-M-Γ of the first Brillouin Zone (see Fig. 6 for the definition) for the $(\pi,0)$ *Ansatz*, $S=0.2$. Left: $\theta=0$, the system has a gap and is a topological spin liquid with short-range $\mathbf{Q}=0$ correlations. The lower band is twofold degenerate corresponding to two different chiralities. Right: $\theta=0.25$, the lower branch becomes gapless at Γ in the thermodynamic limit and gives rise to the Goldstone mode of the long-range Néel order.

of such a spectrum for the *Ansatz* $(\pi,0)$. The spinon band structure is shown in the first Brillouin zone, it has a gap of order $\mathcal{O}(1)$ at point Γ indicative of short-range $\mathbf{Q}=0$ correlations. This gap does not go to zero in the thermodynamic limit: this phase is a disordered topological spin liquid. Adding a Dzyaloshinskii-Moriya perturbation has two effects on the spectrum. It lifts the degeneracy of the lower band corresponding to the symmetry breaking of the model from SU(2) to U(1) and it reduces the gap of the spinon mode that has the chirality opposite to that of the Dzyaloshinskii-Moriya field.

B. Bose-Einstein condensation

With increasing S or θ, the gap decreases and above a critical spin $S_c(\theta)$, the spinon spectrum shows a finite-size gap, which collapses with system size N as $\mathcal{O}(1/N)$. Such a spectrum is shown in Fig. 5 (right). In the thermodynamic limit, the bosons condense in the soft mode (noted $\tilde{\phi}_{\mathbf{q}_0 l_0 \sigma}$ with $\sigma=\uparrow,\downarrow$).[41] This gives a macroscopic contribution to the total number of Schwinger bosons,

$$\frac{1}{2S}\sum_i \langle n_i \rangle = N = \sum_{\mathbf{q}ij} \frac{|V_{\mathbf{q}ij}|^2}{S} = x_{\mathbf{q}_0} N + \sum_{\mathbf{q} \neq \mathbf{q}_0, ij} \frac{|V_{\mathbf{q}ij}|^2}{S}. \tag{14}$$

The condensed fraction $x_{\mathbf{q}_0}$ in the soft mode is of order $\mathcal{O}(1)$ (or equivalently $|V_{\mathbf{q}_0 i l_0}| \sim \sqrt{N}$). The transition to this Bose-Einstein condensed phase corresponds to the development of long-range antiferromagnetic correlations, as can be seen by computing the static structure factor,

$$S^{xx}(\mathbf{Q}) = \frac{3}{4N} \sum_{i,j} e^{i\mathbf{Q}\cdot(\mathbf{R}_i - \mathbf{R}_j)} \langle \tilde{0}|S_i^x S_j^x|\tilde{0}\rangle, \tag{15}$$

where $\mathbf{R}_i$ is the position of site i and x is an axis in the easy plane perpendicular to $\mathbf{D}_{ij}$.

The difference in static structure factor between topological spin-liquid and Néel-ordered phases is illustrated in Fig. 6 for the $(\pi,0)$ *Ansatz* across the Bose-Einstein condensation. In the spin-liquid phase, the structure factor has broad
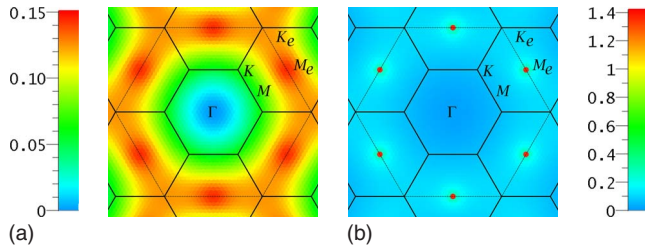
FIG. 6. (Color online) Static structure factor S^{xx} in the extended Brillouin zone for the $(\pi,0)$ state ($\mathbf{Q}=0$) for a lattice size $N=1296$. In the spin-liquid phase $TSL_{\pi,0}$ (left, $S=0.2$, $\theta=0$) there are broad features about $\mathbf{M}_e$ which become peaks with divergent intensity in the ordered phase $LRO_{\pi,0}$ (right, $S=0.2$, $\theta=0.25$).

features located at $\mathbf{Q}=\mathbf{M}_e$ (Fig. 6, left) and at equivalent reciprocal points (these are the Γ points of the second Brillouin zone). This structure factor looks very similar to exact diagonalization and density matrix renormalization group (DMRG) results.[12,37] The features become sharp in the Bose-Einstein condensed phase (Fig. 6, right), where $S^{xx}(\mathbf{M}_e)$ becomes proportional to N,

$$\frac{3}{4N}S^{xx}(\mathbf{M}_e) = m_{AF}^2 + \frac{C^{st}}{\sqrt{N}} + \cdots, \qquad (16)$$

where m_{AF}^2 is the order parameter corresponding to long-range correlations of the 120° $\mathbf{Q}=0$ Néel type.[42] We have extracted m_{AF}^2 by fitting the numerical results (up to $N=1764$) to Eq. (16) with finite-size corrections up to order $1/N$.[43] The extrapolation to the thermodynamic limit of m_{AF}, together with the condensate fraction $x_{\mathbf{q}_0}$ and the gap of the soft spinon are given in Fig. 7 for $S=0.2$. While near the second-order phase transition, the extrapolation of the condensed fraction behaves very smoothly and vanishes right at the point where the gap opens, the extrapolation of the order parameter gives a small shift. We note that m_{AF} is very small (a few percent) in this range of parameters and, therefore, more accurate extrapolations would require using larger system sizes close to the critical point. For strong enough Néel order, however, the two order parameters are clearly proportional ($m_{AF} \propto x_{\mathbf{q}_0}$).
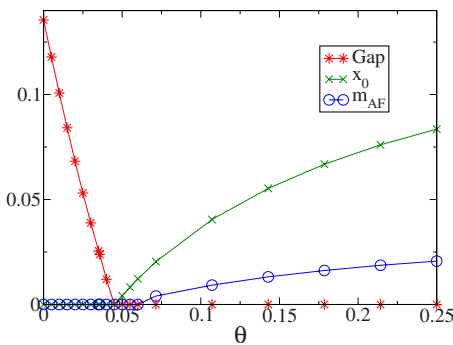

FIG. 7. (Color online) Gap of the soft mode, order parameter m_{AF}, and condensed fraction, $x_{\mathbf{q}_0}$ extrapolated to the thermodynamic limit for the $(\pi,0)$ *Ansatz* as a function of $\theta=D/(2J)(S=0.2)$.
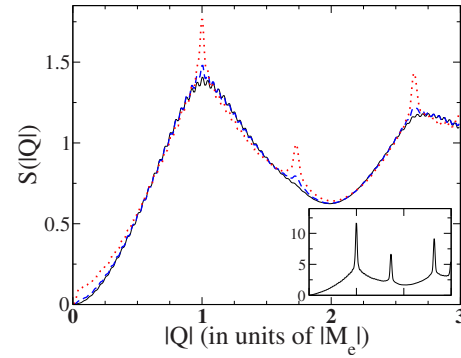

FIG. 8. (Color online) Static structure factor (powder averaged) across the quantum phase transition from the spin liquid to the Néel phase [$S=0.2$ and $\theta=0$ (solid, black), 0.05 (dash, blue), and 0.2 (dot, red)]. Inset: $S=1/2$, $\theta=0$. Small oscillations are finite-size effects.

We have also calculated the static structure factor for powder samples [denoted by $S(|\mathbf{Q}|)$] by averaging Eq. (15) over all directions of $\mathbf{Q}$. In the $(\pi,0)$ spin-liquid phase (Fig. 8 at small D), the overall shape is characteristic of short-range correlations of liquids. We can compare with the calculation of the diffuse scattering for the classical spin-liquid kagomé antiferromagnet by Monte Carlo simulation.[44] Here the position of the first broad peak is at $|\mathbf{M}_e|$ instead of $|\mathbf{K}_e|$ (and the second broad feature is at $\sqrt{7}|\mathbf{M}_e|$). This simply reflects the difference of short-range correlations of the $(\pi,0)$ *Ansatz* and the $\sqrt{3}\times\sqrt{3}$ classical spin liquid. In addition, compared with classical Monte Carlo simulations, we find no intermediate shoulder between the two main broad peaks (except for a little hump at $\sqrt{3}|\mathbf{M}_e|$), a point which seems in fact to be closer to recent experiments on a spin-liquid deuteronium jarosite.[45] Moreover, since the response is due to quantum fluctuations we expect a rather weak sensitivity to the temperature up to temperatures of the order of a fraction of J. When D increases, we see the development of the Bragg peaks in the ordered phase, which increase as the square of the order parameter when we go deep into the ordered phase [Fig. 8 (inset)]. In the ordered phase we can identify two distinct contributions to Eq. (15) by using the sum rule

$$S^{xx}(\mathbf{Q}) = \frac{1}{2\pi}\int d\omega S^{xx}(\mathbf{Q},\omega). \qquad (17)$$

There are the Bragg peaks ($\omega=0$) and also the inelastic collective modes (which we will detail below) which give the additional magnetic background scattering (which is the only contribution to scattering in the spin-liquid phase). It is noteworthy that the latter is relatively strong for low spin (Fig. 8) and becomes relatively much smaller once the order parameter is large (inset of Fig. 8). In fact the transfer of spectral weight from the magnetic continuum background to the Bragg peaks goes as the square of the order parameter. Note also that $S(|\mathbf{Q}|)$ does not vanish any more for small $\mathbf{Q}$ at $D \neq 0$, this is because in the presence of the anisotropy the ground state is no longer an SU(2) singlet. Although the effect is small the measurement at small $|\mathbf{Q}|$ in the spin-
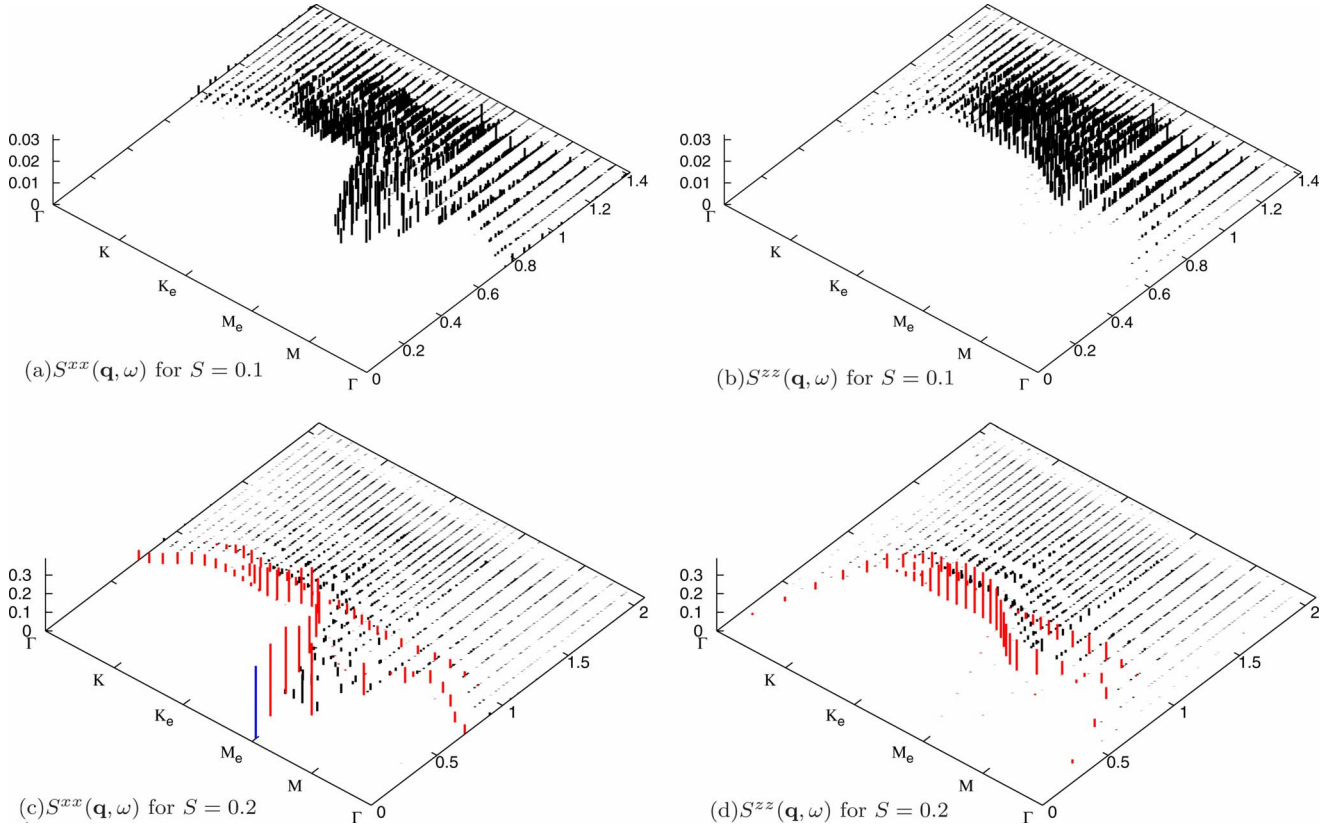
FIG. 9. (Color online) Dynamical structure factors $S^{xx}(\mathbf{q},\omega)$ and $S^{zz}(\mathbf{q},\omega)$ for the $\mathbf{Q}=0$ *Ansatz* in the spin-liquid phase, $S=0.1$ or with long-range order, $S=0.2$. The system size is $N=576$. θ is taken to be 0.25 to emphasize the anisotropy of $S^{xx}(\mathbf{q},\omega)$ and $S^{zz}(\mathbf{q},\omega)$. In the Néel phase, the largest peak (in blue online) is the quasielastic peak, next in intensity are the magnon branches (in red online) (intensities are cut to see the weaker continuum).

liquid phase could help to figure out what the anisotropy is (or give an upper bound when the signal is small, see, e.g., Ref. 46). In the ordered phase, the finite uniform susceptibility should give a finite contribution at $\mathbf{Q}=0$ but we recall that this contribution is absent for the U(1) singlet ground state of Schwinger-boson theory.

V. DYNAMICAL SPIN STRUCTURE FACTOR

The Schwinger-boson approach allows to calculate the dynamical response of the system, which is interesting both theoretically and for a direct comparison with experiments. The inelastic neutron cross section is proportional to the spin dynamical structure factor

$$S^{\alpha\alpha}(\mathbf{Q},\omega) = \int_{-\infty}^{+\infty} dt\, e^{i\omega t}\langle S^{\alpha}_{-\mathbf{Q}}(t) S^{\alpha}_{\mathbf{Q}}(0)\rangle, \quad (18)$$

$$= 2\pi \sum_{p} |\langle p|S^{\alpha}_{\mathbf{Q}}|\tilde{0}\rangle|^2 \delta(\omega - \omega_p), \quad (19)$$

where $\alpha = x, y, z$ depending on the polarization of the incident neutrons, $|\tilde{0}\rangle$ is the ground state, and

$$\mathbf{S}_{\mathbf{Q}} = \sqrt{\frac{3}{4N}} \sum_{\mathbf{x}i} e^{-i\mathbf{Q}\cdot\mathbf{R}_{i\mathbf{x}}} \mathbf{S}_{i\mathbf{x}} \quad (20)$$

with $\mathbf{R}_{i\mathbf{x}}$ the position of the site $i\mathbf{x}$. We use the Fourier transform and the Bogoliubov transformation to express $\mathbf{S}_{\mathbf{Q}}$ in terms of quasiparticle operators [Eq. (10)]. At zero temperature, since $|\tilde{0}\rangle$ is the vacuum of quasiparticles, only creation operators are retained. Given that $\mathbf{S}_{i\mathbf{x}}$ is quadratic in boson operators, we can only create spinons by pair. For example, the following term is present in $S^z_{\mathbf{Q}}$:

$$\sum_{\mathbf{q}ln} U^*_{\mathbf{q}il} V_{(\mathbf{q}+\mathbf{Q})in} (\tilde{a}_{l\mathbf{q}})^\dagger (\tilde{b}_{n-(\mathbf{q}+\mathbf{Q})})^\dagger, \quad (21)$$

which applied to $|\tilde{0}\rangle$ in the matrix element [Eq. (19)] creates a pair of spinons $|p\rangle$ with energy $\omega_p = \omega_{\mathbf{q}l} + \omega_{-(\mathbf{q}+\mathbf{Q})n}$ and wave vector $-\mathbf{Q}$. The intensity of the transition is obtained by computing the product of matrices such as in Eq. (21) for each pair of modes.

We now discuss the general features of the dynamical spin structure factor and show the results for the $\mathbf{Q}=0$ *Ansatz* in Fig. 9. In the spin-liquid phase $[S<S_c(\theta)]$, all spinons are gapped and the two-spinon excitations form a gapped continuum, the bottom edge of which is given by the minimum of $\omega_{\mathbf{q}l} + \omega_{-(\mathbf{q}+\mathbf{Q})n}$ over all $\mathbf{q}$ and all spinon bands (l,n). $S^{xx}(\mathbf{Q},\omega)$ and $S^{zz}(\mathbf{Q},\omega)$ are given in Figs. 9(a) and 9(b). In

these figures, we have taken D large enough to see the anisotropy of the response (and a small $S=0.1$ to be in the spin-liquid phase). When S increases the lower edge of the continuum shifts to zero and its intensity increases continuously.

For $S>S_c(\theta)$ [Figs. 9(c) and 9(d), $S=0.2$, $\theta=0.25$], due to the soft spinon mode $\tilde{\phi}_{\mathbf{q}_0 l_0 \sigma}$ [see Fig. 5 (right)] the system enters a Bose-condensed phase: it has long-range correlations and low-energy excitations varying as $1/N$, at $\mathbf{M}_e$. This spinon mode has a singular contribution $\sim \sqrt{N}$ [see Eq. (14)]. As a consequence, the intensities have different finite-size scaling, depending on whether the pair of excited spinons contains the soft spinon or not. We can therefore identify three contributions.

Elastic peak. This is the peak with the largest intensity at $\mathbf{Q}=\mathbf{M}_e$ [shown in blue (online) in Fig. 9(c) and cut in intensity to show the other excitations]. It comes from a pair of (identical) soft spinons (with wave vector $\mathbf{q}_0=0$) in Eq. (21) and so has energy $\mathcal{O}(1/N)$ and intensity proportional to $|U_{\mathbf{q}_0 i l_0} V_{\mathbf{q}_0 i l_0}/\sqrt{N}|^2 \sim N$. By integrating over all frequencies, only this (zero-frequency) peak contributes to the peak of the (equal-time) structure factor, $S^{xx}(\mathbf{M}_e)$ [Fig. 6 (right)]. We also note that the peak is absent in the zz response [Fig. 9(d)], which is expected because the correlations are long ranged in the plane only.

Magnon branches. There are three magnon branches [shown in red (online) in Figs. 9(c) and 9(d)], two are "optical" modes, the third one, gapless, is the Goldstone mode of the U(1) symmetry. The (almost) flat mode is the *weathervane mode* which is always gapped in the Schwinger-boson approach, contrary to spin-wave theory,[47] and irrespective of S.[28] The magnon here consists of a pair of the soft spinon and a spinon of wave vector $\mathbf{Q}$ [see Eq. (21)] so that the magnon dispersion *is* the spinon dispersion $\omega_{\mathbf{Q}\mu}$ (Ref. [48]) and the intensities are of order $|U_{\mathbf{q} i n} V_{\mathbf{q}_0 i l_0}/\sqrt{N}|^2 \sim 1$.

Continuum. As for the spin-liquid phase, there is a continuum of excitations obtained from contributions in Eq. (21) with two spinons both different from the soft mode. Each peak has intensity $|U_{\mathbf{q} i n} V_{\mathbf{k} i l}/\sqrt{N}|^2 \sim \mathcal{O}(1/N)$ and the sum of them gives a continuum with finite intensity in the thermodynamic limit, which is absent in lowest-order spin-wave theory.

All these excitations contribute to the sum rule, $N\langle(S_i^x)^2\rangle = \Sigma_q \int (d\omega/2\pi) S^{xx}(q,\omega)$, given the different density of states. Note that, as expected, the Dzyaloshinskii-Moriya interaction introduces an anisotropy between the in-plane [Figs. 9(a) and 9(c)] and the out-of-plane [Figs. 9(b) and 9(d)] dynamical factors. This anisotropy is visible in the spin-liquid as well as in the Néel-ordered phase. The effect is more spectacular in the latter where the Dzyaloshinskii-Moriya interaction strongly suppresses the low-energy response in the zz channel around the $\mathbf{M}_e$ point.

VI. CONCLUSION

We have obtained the Schwinger-boson mean-field phase diagram for different values of S. The large S limit is in agreement with the semiclassical order by disorder mechanism which selects the $\sqrt{3}\times\sqrt{3}$ state.[28] We find that this phase remains stable at small anisotropy in a region which becomes broader and broader when the spin decreases (and hence quantum-mechanical effects increase). It is therefore possible in principle to observe both ordered phases experimentally and first-order transitions between them. However, given the small critical strength, the $\mathbf{Q}=0$ phase is more likely to occur in a real compound with large enough S and the kagome potassium jarosite ($S=5/2$) offers such an example.[49,50]

We have identified a region of the phase diagram [$S \sim 0.2$, *Ansatz* $(\pi,0)$] which resembles qualitatively to the exact diagonalization results for the $S=1/2$ system, where the Dzyaloshinskii-Moriya interaction induces a quantum phase transition between a topological spin liquid and the $\mathbf{Q}=0$ Néel-ordered phase. This suggests to consider smaller values of the "spin" parameter S as possibly relevant within the Schwinger-boson theory, given that the treatment on average of the constraint leads to enhance $\langle \mathbf{S}_i^2 \rangle$ compared to $S(S+1)$. Within this framework, we could calculate observables such as (i) the cross section of diffuse neutron scattering, with the evolution from broad diffuse scattering to Bragg peaks across the quantum phase transition (Figs. 6 and 8) and (ii) the neutron inelastic cross section which, in addition to Bragg peaks and spin waves, shows a broad continuum in both disordered and ordered phases (Fig. 9), absent in the lowest-order of spin-wave theory.

[1] I. Dzyaloshinskii, J. Phys. Chem. Solids **4**, 241 (1958); T. Moriya, Phys. Rev. **120**, 91 (1960).

[2] N. Read and S. Sachdev, Phys. Rev. Lett. **66**, 1773 (1991).

[3] X. G. Wen, Phys. Rev. B **44**, 2664 (1991).

[4] G. Misguich and C. Lhuillier, in *Frustrated Spin Systems*, edited by H. T. Diep (World Scientific, Singapore, 2005).

[5] O. Cépas, K. Kakurai, L. P. Regnault, T. Ziman, J. P. Boucher, N. Aso, M. Nishi, H. Kageyama, and Y. Ueda, Phys. Rev. Lett. **87**, 167205 (2001).

[6] P. Sindzingre and C. Lhuillier, EPL **88**, 27009 (2009).

[7] M. B. Hastings, Phys. Rev. B **63**, 014413 (2000).

[8] Y. Ran, M. Hermele, P. A. Lee, and X.-G. Wen, Phys. Rev. Lett. **98**, 117205 (2007).

[9] S. Ryu, O. I. Motrunich, J. Alicea, and M. P. A. Fisher, Phys. Rev. B **75**, 184406 (2007).

[10] P. Lecheminant, B. Bernu, C. Lhuillier, L. Pierre, and P. Sindzingre, Phys. Rev. B **56**, 2521 (1997).

[11] C. Waldtmann, H.-U. Everts, B. Bernu, C. Lhuillier, P. Sindzin-

gre, P. Lecheminant, and L. Pierre, Eur. Phys. J. B **2**, 501 (1998).

[12] H. C. Jiang, Z. Y. Weng, and D. N. Sheng, Phys. Rev. Lett. **101**, 117203 (2008).

[13] R. R. P. Singh and D. A. Huse, Phys. Rev. B **77**, 144415 (2008).

[14] P. Mendels, F. Bert, M. A. de Vries, A. Olariu, A. Harrison, F. Duc, J. C. Trombe, J. S. Lord, A. Amato, and C. Baines, Phys. Rev. Lett. **98**, 077204 (2007).

[15] J. S. Helton, K. Matan, M. P. Shores, E. A. Nytko, B. M. Bartlett, Y. Yoshida, Y. Takano, A. Suslov, Y. Qiu, J.-H. Chung, D. G. Nocera, and Y. S. Lee, Phys. Rev. Lett. **98**, 107204 (2007).

[16] M. A. de Vries, K. V. Kamenev, W. A. Kockelmann, J. Sanchez-Benitez, and A. Harrison, Phys. Rev. Lett. **100**, 157205 (2008).

[17] M. A. de Vries, J. R. Stewart, P. P. Deen, H. M. Ronnow, and A. Harrison, Phys. Rev. Lett. **103**, 237201 (2009).

[18] G. Misguich and P. Sindzingre, Eur. Phys. J. B **59**, 305 (2007).

[19] T. Imai, E. A. Nytko, B. M. Bartlett, M. P. Shores, and D. G. Nocera, Phys. Rev. Lett. **100**, 077203 (2008).

[20] A. Olariu, P. Mendels, F. Bert, F. Duc, J. C. Trombe, M. A. de Vries, and A. Harrison, Phys. Rev. Lett. **100**, 087202 (2008).

[21] M. Rigol and R. R. P. Singh, Phys. Rev. Lett. **98**, 207204 (2007); Phys. Rev. B **76**, 184403 (2007).

[22] A. Zorko, S. Nellutla, J. van Tol, L. C. Brunel, F. Bert, F. Duc, J. C. Trombe, M. A. de Vries, A. Harrison, and P. Mendels, Phys. Rev. Lett. **101**, 026405 (2008).

[23] O. Cépas, C. M. Fong, P. W. Leung, and C. Lhuillier, Phys. Rev. B **78**, 140405(R) (2008).

[24] I. Rousochatzakis, S. R. Manmana, A. M. Läuchli, B. Normand, and F. Mila, Phys. Rev. B **79**, 214415 (2009).

[25] M. Hermele, Y. Ran, P. A. Lee, and X.-G. Wen, Phys. Rev. B **77**, 224413 (2008).

[26] P. W. Leung and V. Elser, Phys. Rev. B **47**, 5459 (1993).

[27] A. Auerbach and D. P. Arovas, Phys. Rev. Lett. **61**, 617 (1988).

[28] S. Sachdev, Phys. Rev. B **45**, 12377 (1992).

[29] L. O. Manuel, C. J. Gazza, A. E. Trumper, and H. A. Ceccatto, Phys. Rev. B **54**, 12946 (1996).

[30] S. Sarker, C. Jayaprakash, H. R. Krishnamurthy, and M. Ma, Phys. Rev. B **40**, 5028 (1989).

[31] F. Wang and A. Vishwanath, Phys. Rev. B **74**, 174423 (2006).

[32] O. Tchernyshyov, R. Moessner, and S. L. Sondhi, Europhys. Lett. **73**, 278 (2006).

[33] J.-C. Domenge, P. Sindzingre, C. Lhuillier, and L. Pierre, Phys. Rev. B **72**, 024433 (2005).

[34] J. H. P. Colpa, Physica A **93**, 327 (1978).

[35] This fact was already mentioned implicitly by T. Yavors'kii, W. Apel, and H.-U. Everts, Phys. Rev. B **76**, 064430 (2007).

[36] M. Elhajal, B. Canals, and C. Lacroix, Phys. Rev. B **66**, 014422 (2002).

[37] A. Laeuchli and C. Lhuillier, arXiv:0901.1065 (unpublished).

[38] A simple way to derive the 3/2 factor (see, however, A. Auerbach, *Interacting Electrons and Quantum Magnetism* (Springer-Verlag, Berlin, 1994 for the discussion of the $1/\mathcal{N}$ corrections) is to use the Wick theorem: $\langle n_i^2 \rangle - \langle n_i \rangle^2 = \langle n_{ai} \rangle (\langle n_{ai} \rangle + 1) + \langle n_{bi} \rangle (\langle n_{bi} \rangle + 1) + |\langle a_i^2 \rangle|^2 + |\langle b_i^2 \rangle|^2 + 2|\langle a_i b_i \rangle|^2 + 2|\langle a_i^\dagger b_i \rangle|^2$. At $D=0$, the Hamiltonian is SU(2) invariant and we obtain $\langle n_i^2 \rangle - \langle n_i \rangle^2 = 2S(S+1)$. For $D \neq 0$, $\langle a_i b_i \rangle \neq 0$.

[39] At finite $\mathcal{N}$ and for sufficiently small boson density, the problem is strictly equivalent to gapped spinons (the Schwinger bosons) interacting with a fluctuating bond field. It has been understood that the low-energy physics of such a system will be that of a lattice gauge theory coupled to charged matter fields. But the nature (group) of the gauge field crucially depends on the lattice geometry and in the present case where the lattice is not bipartite, it should generically be of $\mathbb{Z}_2$ type and has two types of phases (Refs. 2 and 40). If the effective $\mathbb{Z}_2$ gauge theory is in a deconfined phase (which should be the case for large enough $\mathcal{N}$), the ground state is qualitatively close to the mean-field one, with gapped and unconfined spinons. If the phase is instead confined, the gauge fluctuations are strong and cannot be neglected, the mean-field picture is not valid any more.

[40] G. Misguich, arXiv0809 (unpublished). Lectures given at the Les Houches summer school on *Exact Methods in Low-Dimensional Statistical Physics and Quantum Computing*, 2008.

[41] For the sake of simplicity we develop only the formulas corresponding to a unique soft mode. This is the case of the Néel order in presence of a Dzyaloshinskii-Moriya interaction: due to the U(1) symmetry of the original Hamiltonian, the Goldstone mode is unique. The general case is straightforward but more cumbersome in writing.

[42] m_{AF}^2 is delicate to normalize because of the fluctuations of the spin length on each site. Fluctuations also increase with the strength of the Dzyaloshinskii-Moriya coupling, making the normalization partly arbitrary.

[43] H. Neuberger and T. Ziman, Phys. Rev. B **39**, 2608 (1989); D. S. Fisher, *ibid.* **39**, 11783 (1989); P. Hasenfratz and F. Niedermayer, Zeitschrift für Physik B **92**, 91 (1993).

[44] J. N. Reimers, Phys. Rev. B **46**, 193 (1992).

[45] B. Fåk, F. C. Coomer, A. Harrison, D. Visser, and M. E. Zhitomirsky, EPL **81**, 17006 (2008).

[46] S.-H. Lee, C. Broholm, G. Aeppli, A. P. Ramirez, T. G. Perring, C. J. Carlile, M. Adams, T. J. L. Jones, and B. Hessen, Europhys. Lett. **35**, 127 (1996).

[47] A. B. Harris, C. Kallin, and A. J. Berlinsky, Phys. Rev. B **45**, 2899 (1992).

[48] If $\mathbf{q}_0 \neq 0$, the spinon dispersion is folded in the magnetic Brillouin zone.

[49] A. S. Wills, Phys. Rev. B **63**, 064430 (2001).

[50] For $S > 1/2$, we note that single-ion anisotropies are also present and may affect the form of magnetic order.